Article

RAFT Polymer-Based Surfactants for Minerals Recovery

Negin Amini,[||] Bo Fan,[||] Tina Hsia, Ellen M. Moon,* Karen Hapgood, and San H. Thang*

Read Online

ACCESS | Metrics & More | Article Recommendations | SI Supporting Information

ABSTRACT: Reagent consumption is an ongoing sustainability challenge for the mineral processing industry. There is a need to recover, regenerate, and reuse as many of the chemical inputs as possible. This study investigated the design and synthesis via reversible addition−fragmentation chain transfer (RAFT) polymerization of a novel polymer for use as a surfactant in a water-in-oil (w/o) emulsion system for ultrafine minerals recovery. The polymers were designed to hold a thermoresponsive moiety to allow for future recovery. The performance of the novel emulsion was tested for agglomeration of ultrafine talc mineral particles. A traditional emulsion containing sorbitan monooleate as the surfactant was used as a research benchmark to compare against the novel emulsion's stability and performance in minerals recovery. The novel RAFT polymer-based emulsions formed large and stable water droplets surrounded by a halo of smaller water droplets. Over time, the smaller droplets coalesced and a more uniform size distribution of droplets was formed, keeping the emulsion stable. Rheological testing of freshly made and aged emulsions showed both traditional and novel emulsions to have a high viscosity at a low shear rate. RAFT polymer B with a hydrophilic−lipophilic block ratio of 5:10 performed adequately as a surfactant replacement to stabilize w/o emulsions. The mineral recovery using the novel emulsion was on par with the traditional emulsions. The novel RAFT emulsion containing 2.5 wt % polymer B achieved 90% minerals recovery, a similar yield to the traditional emulsions. This study demonstrates that surfactants containing stimuli-responsive moieties can be synthesized via RAFT polymerization and successfully used in mineral processing applications to recover ultrafine particles. Work is ongoing to exploit the stimuli responsiveness to recover the polymer surfactant for reuse.
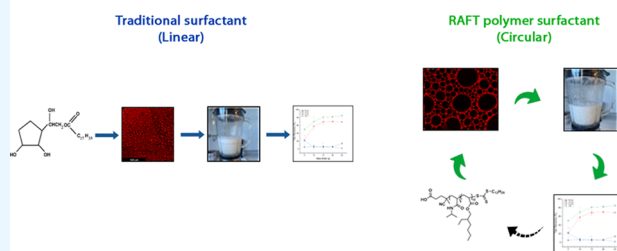
1. INTRODUCTION

The demand to extract valuable metals from mineral ores has increased over the past 100 years.[1] With lower ore grades, more complex deposits, and challenges associated with the cost and supply of energy and water,[2] there is an urgent need for new recovery techniques that are both highly selective and environmentally sustainable. The traditional minerals processing technique of froth flotation consumes not only significant amounts of energy but also chemical collectors to selectively recover hydrophobic particles to produce valuable metals.[3] By the end of 2027, the global market for collectors used in minerals processing is forecasted to reach a value of over US $100 billion.[4] Furthermore, froth flotation has a limitation where it cannot capture ultrafine particles that are below the hydrodynamic limit of flotation. An innovative new technique is required, which retrieves the collectors and minimizes energy requirement, for fast recovery of the ultrafine mineral particles.

The principle of oil agglomeration[5] which has been used for carbonaceous materials can also be applied to ultrafine mineral particles as an alternative to froth flotation. However, the relatively large amount of oil necessary prevents the industrial adoption of this process. To address this, research has been carried out using water-in-oil emulsions with the addition of a surfactant to keep the immiscible phases from separating. At least 10 vol % oil is required to achieve agglomeration on an industrial scale, making the process unfeasible. A study by van Netten et al. in 2017 investigated selective agglomeration using high internal phase (HIP) emulsion binder to achieve beneficiation using fine coal particles. Selective agglomeration was achieved and improved with 3 wt % aqueous NaCl solution, reducing the Ostwald ripening effect that occurs in the emulsion and reducing the oil requirement by 7-fold. A subsequent study[6] used the same HIP emulsion binder with ultrafine hydrophobic mineral particles and achieved agglomeration within seconds. A study by Hornn et al. used anionic surfactants potassium amyl xanthate (KAX) for the stabilization of oil−water emulsions for the recovery of copper in agglomeration-flotation of chalcopyrite and quartz. The prepared emulsions had smaller oil droplets as the dispersed phase and recovered ∼83% of the copper from the system.[7] Sahasrabudhe et al. also investigated HIP emulsions for

selective chalcopyrite recovery. Emulsification of kerosene/water mixtures was prepared and stabilized by sodium isobutyl xanthate (SIBX) collectors. The optimum chemistry conditions were a pH of 8.5 to 9.5, reaching copper recovery of up to 98%.[8] In all of the case studies above, the emulsions cannot be recovered.

As shown in recent studies,[6,9] HIP water-in-oil emulsions can achieve near-complete recovery of hydrophobized mineral particles. While oil adhesion is still the process driving the agglomeration, the nature of the thin film oils (∼30 nm) within the HIP emulsion and their ability to efficiently deliver the organic liquid to the particle surface mean that the process can occur with lower overall concentrations of oil.[10] The mechanism by which oil binds hydrophobic particles is akin to spherical agglomeration, where a bridging liquid joins two, and then progressively more, particles.[10] Early reports describing the mechanism of spherical agglomeration were based on the dewatering of slurry systems containing fine particles,[11] with more recent comparison of the mechanism made to wet granulation.[12] The agglomeration mechanism is broken down into the following categories: nucleation, growth, and breakage.[12]

In the scenario for minerals processing, the emulsion binder and the mineral particle are brought together to form a nuclei granule, and the collisions in the mixer will promote growth by layering to form a larger granule. Because the agglomeration requires the HIP emulsion to remain somewhat intact, the granules will break down with the application of high shear or extending the collision time. The system will be in this equilibrium, and the granules will continue to break to smaller granules and revert to larger granules.

Emulsions require surfactants to reduce the interfacial tension and stabilize the system. Traditionally short-chain surfactants in emulsions have been vastly reported in the literature. In one study, Fu et al. reported individual and combinations of Tween80, OP10, Span80, and Span85 for the emulsification of water/octane mixtures.[13] The optimal conditions were reported to be mixed surfactant systems with a hydrophilic–lipophilic balance (HLB) value of 9 to produce emulsions with 200 nm dispersed water droplets. Another study by John et al. investigated the emulsification of vegetable oil/water mixtures stabilized by several short-chained surfactants: Tween40, Tween60, polyoxyethylene (20) sorbitan monopalmitate, and polyoxyethyelene (20) monostearate (nonionic). They produced phase diagrams for each emulsion system to determine the limit for the thermodynamically stable phases, to help identify the isotropic emulsion regions, and to predict the correct amount of emulsions needed for mixing to obtain an emulsion.[14]

There have been several reports in the literature that investigate sustainably derived polymer surfactants. A study by Ghavidel and Fatehi investigated the mechanism of adsorption and interfacial behavior of sulfonated polymeric lignin, a biobased polymer, for use as a surfactant to stabilize the oil/water interface in emulsions.[15] The emulsifying performance was dependent on adsorption at the oil/water interface. Another study by Kang et al. reported synthetic polymers as surfactant in w/o emulsions that form stable emulsions with the degree of polymer influencing the emulsion stability.[16] The idea of using synthetic polymers as surfactants allows for tailoring of structures to suit a specific system or purpose and requires further investigation.

Reversible addition–fragmentation chain transfer (RAFT) polymerization is a technique that is used to synthesize polymers with a high degree of control over polymer structure and molecular weights.[17−19] It uses thiocarbonylthio compounds as the RAFT agents and is suitable for synthesizing homopolymer; gradient, diblock, triblock, and star polymers; and more complex systems such as polymer-based nano/microparticles.[20−24] In a study by Thompson et al.,[25] RAFT-mediated polymerization-induced self-assembly (RAFT-PISA) technique was used to prepare various amphiphilic block copolymer nanoparticles as Pickering emulsifiers. It was used for the stabilization of the n-dodecane-in-water emulsions. The linear diblock polymers and worms did not survive the high shear homogenization for emulsification. The copolymer acts as a surfactant to produce a stable emulsion and is adsorbed onto the oil–water interface. The weakly lipophilic nature of the copolymer leads to particle dissociation during the emulsification but can be stabilized with the addition of ethylene glycol dimethacrylate to cross-link the particles. Alternatively, replacing or supplementing the copolymer with more hydrophobic functional groups can achieve stabilization.

Given the ability to finely tailor the chemistry of RAFT polymers, there has been recent interest in their use in minerals processing where selectivity is required, for example, as floatation agents and for selective ion adsorption.[26,27] Further, the RAFT polymerization process allows for the insertion of stimuli-responsive moieties that allow the polymer to have different properties under different stimuli. Poly(N-isopropylacrylamide), abbreviated as PNIPAM, displays a temperature-responsive change in water solubility. The polymer exhibits a lower critical solution temperature (LCST); below this point, the polymer is in extended state, and above the LCST, it collapses into a globule form due to lower solubility.[28−30] This interesting property has allowed its use in a range of advanced applications, such as smart nanodelivery systems, selective membrane gate, and responsive hydrogels.[31−33]

The aim of this study was to determine whether custom-designed polymers can be used to replace the surfactants in the emulsion and ultimately be recovered for reuse. This study therefore seeks to develop a solution to target mineral recovery that addresses the issue of reagent consumption. We aim to design, synthesize via RAFT polymerization, and test the efficacy of a series of novel polymers as surfactants in a w/o emulsion binder for ultrafine minerals recovery. Crucially, the polymers contain PNIPAM, which has been shown to be thermoresponsive in water. Demonstrating the efficacy of such polymers in facilitating the oil agglomeration process is the first step toward the design of polymers that can be recovered and reused in mineral processing.

2. EXPERIMENTAL SECTION

2.1. Materials. N-Isopropylacrylamide 98% (NIPAM) was purchased from AK Scientific. 2-Ethylhexyl acrylate 98% (2EHA) was purchased from Sigma-Aldrich. 4-Cyano-4-(((dodecylthio)carbonothioyl)thio) pentanoic acid 97% (CDPA) was purchased from Boron Molecular (Australia). 2,2′-Azobis(isobutyronitrile) (AIBN) was purchased from FUJIFILM Wako Chemicals. AIBN was recrystallized from ethanol and then stored in a freezer at −20 °C. 1,4-Dioxane was purchased from Ajax Finechem. 2EHA was purified by passing through a basic Al_2O_3 (pore size 0.063−0.20 mm, Merck) column before use.
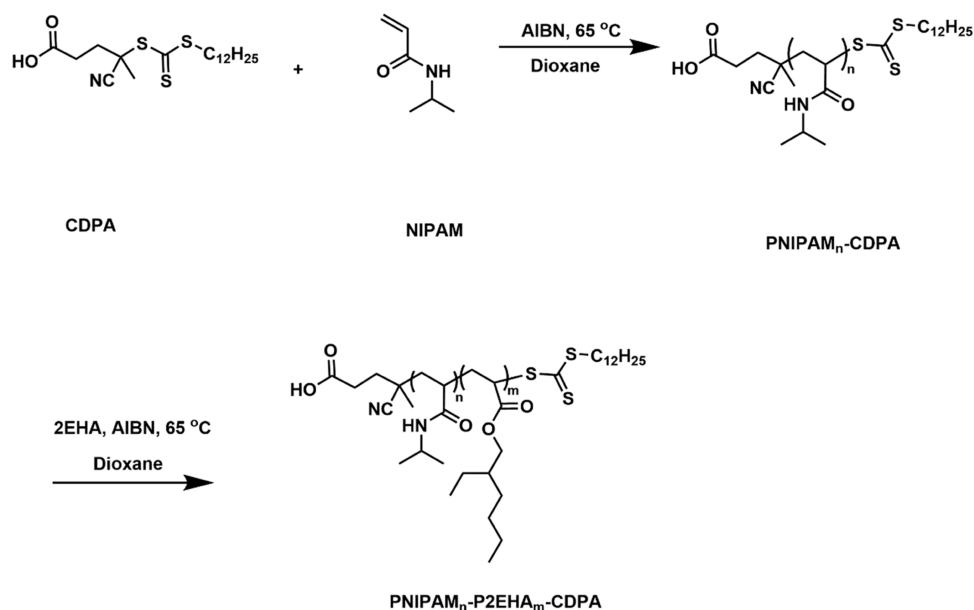
Figure 1. Synthesis procedure for the block copolymers PNIPAM$_n$-b-P2EHA$_m$-CDPA.

Industrial talc was sourced from Barnes (manufacturer, Liaoning Aihai Talc Co. Ltd.) and used for agglomeration experiments. Low-odor kerosene oil (Diggers) was sourced from Bunnings Warehouse, and nonionic surfactant (sorbitan monooleate which is commercially available from Sigma-Aldrich as Span80) was used to make the traditional water-in-oil emulsion binders.

2.1.1. Design and Synthesis of RAFT Polymers for Surfactant-Based Applications. Polymers (A–D) were synthesized in two steps: first, precursors PNIPAM$_n$-CDPA with predetermined repeating units were synthesized under the control of RAFT agent CDPA, and the precursors were then used directly to synthesize the final block copolymers (PNIPAM$_n$-b-P2EHA$_m$-CDPA) with the addition of second monomer 2EHA (Figure 1).

2.1.1.1. Synthesis of PNIPAM$_5$-CDPA. CDPA (2.86 g, 7.08 mmol, 1.0 equiv), NIPAM (4.00 g, 35.34 mmol, 5.0 equiv), and AIBN (116.0 mg, 707 μmol, 0.1 equiv) were dissolved in 6.0 mL of 1,4-dioxane and transferred to a Schlenk flask. The oxygen was removed by 3 cycles of freeze−pump−thaw and refilled with argon in the third cycle. The reaction was stopped by cooling down to room temperature after being immersed in a 65 °C oil bath for 24 h. The polymer was used directly for the next step. ^{1}H NMR (400 MHz, CDCl$_3$): δ 5.88−6.78 (b, 5H), 4.48−4.73 (b, 2H), 3.90−4.19 (b, 6H), 1.60−2.67 (b, 20H), 1.05−1.47 (b, 53H), 0.87 (t, J = 7.09 Hz, 3H).

2.1.1.2. Synthesis of PNIPAM$_2$-CDPA. CDPA (6.00 g, 14.86 mmol, 1.0 equiv), NIPAM (3.36 g, 29.72 mmol, 2.0 equiv), and AIBN (122.0 mg, 743 μmol, 0.05 equiv) were dissolved in 6.0 mL of 1,4-dioxane and transferred to a Schlenk flask. The oxygen was removed by 3 cycles of freeze−pump−thaw and refilled with argon in the third cycle. The reaction was stopped by cooling down to room temperature after being immersed in a 65 °C oil bath for 24 h. The polymer was used directly for the next step. ^{1}H NMR (400 MHz, CDCl$_3$): δ 5.87−6.86 (b, 2H), 4.48−4.71 (b, 1H), 3.94−4.18 (b, 2H), 1.60−2.76 (b, 11H), 1.05−1.47 (b, 33H), 0.87 (t, J = 7.09 Hz, 3H).

2.1.1.3. Synthesis of PNIPAM$_5$-b-P2EHA$_5$-CDPA (Polymer A). PNIPAM$_5$-CDPA (3.43 g, 3.54 mmol, 1.0 equiv), 2EHA (3.26 g, 17.4 mmol, 5.0 equiv), and AIBN (58.0 mg, 354 μmol,

0.1 equiv) were dissolved in 5.0 mL of 1,4-dioxane and transferred to a Schlenk flask. The oxygen was removed by 3 cycles of freeze−pump−thaw and refilled with argon in the third cycle. The reaction was stopped by cooling down to room temperature after being immersed in a 65 °C oil bath for 24 h. The polymer was dried by blowing with air and further dried under high vacuum for 24 h. ^{1}H NMR (400 MHz, CDCl$_3$): δ 5.62−7.01 (b, 5H), 4.71−4.95 (b, 1H), 3.72−4.65 (b, 14H), 3.26−3.40 (b, 2H), 1.45−2.60 (b, 35H), 1.05−1.47 (b, 83H), 0.75−0.97 (b, 29H).

2.1.1.4. Synthesis of PNIPAM$_5$-b-P2EHA$_{10}$-CDPA (Polymer B). This polymer was synthesized in a procedure similar to that for Polymer A by varying the monomer stoichiometry. ^{1}H NMR (400 MHz, CDCl$_3$): δ 5.64−6.95 (b, 5H), 4.71−4.91 (b, 1H), 3.72−4.26 (b, 22H), 3.19−3.40 (b, 2H), 1.47−2.62 (b, 50H), 0.98−1.47 (b, 113H), 0.78−0.97 (b, 51H). GPC (THF, PS standards): M_n = 2700 g/mol, Đ = 1.22.

2.1.1.5. Synthesis of PNIPAM$_2$-b-P2EHA$_2$-CDPA (Polymer C). This polymer was synthesized in a procedure similar to that for Polymer A by varying the monomer stoichiometry. ^{1}H NMR (400 MHz, CDCl$_3$): δ 5.67−6.73 (b, 2H), 4.77−4.99 (b, 1H), 3.82−4.22 (b, 5H), 3.26−3.46 (b, 2H), 1.46−2.72 (b, 16H), 1.01−1.46 (b, 38H), 0.78−1.01 (b, 11H). GPC (THF, PS standards): M_n = 1200 g/mol, Đ = 1.08.

2.1.1.6. Synthesis of PNIPAM$_2$-b-P2EHA$_5$-CDPA (Polymer D). This polymer was synthesized in a procedure similar to that for Polymer A by varying the monomer stoichiometry. 1H NMR (400 MHz, CDCl$_3$): δ 5.73−6.75 (b, 2H), 4.73−4.95 (b, 1H), 3.83−4.23 (b, 9H), 3.20−3.43 (b, 2H), 1.48−2.69 (b, 23H), 1.01−1.47 (b, 53H), 0.77−0.97 (b, 23H). GPC (THF, PS standards): M_n = 1700 g/mol, Đ = 1.21.

2.1.1.7. Polymer design rationale. The design and selection of surfactants are critical for forming stable HIP emulsions. Typically, the formation of stable HIP emulsions requires the addition of low-molecular-weight surfactants or the addition of solid colloidal particles in the continuous phase to form Pickering HIP emulsions.[34] Furthermore, the formation of water-in-oil or oil-in-water emulsion is also dictated by the properties of surfactants, and generally, if the surfactant is predominantly soluble in the oil phase, a water-in-oil emulsion
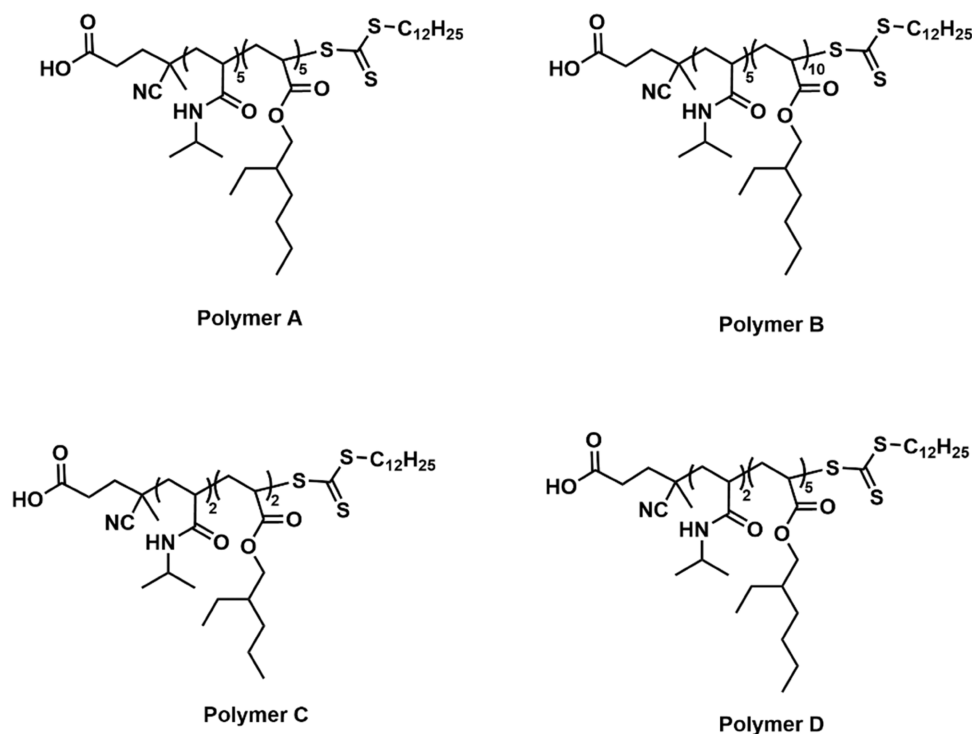
Figure 2. Molecular structures for the oil-soluble polymers (A–D) synthesized via RAFT polymerization. The hydrophilic–lipophilic ratios for each: Polymer A (5–5), Polymer B (5–10), Polymer C (2–2), and Polymer D (2–5).

Table 1. Summary of the Polymer-Based Surfactant Synthesized by RAFT Polymerization

	structural formulas[a]	conv. (%)[b]	$M_{n,theo}$ (g/mol)[c]	$M_{n,calc}$ (g/mol)[d]	GPC[e]		
					M_n (g/mol)[f]	M_w (g/mol)[g]	Đ[h]
Polymer A	PNIPAM$_5$-b-P2EHA$_5$-CDPA	>99	1891	1800			
Polymer B	PNIPAM$_5$-b-P2EHA$_{10}$-CDPA	>99	2813	2500	2700	3300	1.22
Polymer C	PNIPAM$_2$-b-P2EHA$_2$-CDPA	>99	999	900	1200	1300	1.08
Polymer D	PNIPAM$_2$-b-P2EHA$_5$-CDPA	>99	1552	1400	1700	1900	1.21

[a]Target polymer structural formulas according to monomers addition stoichiometry. [b]The monomer conversions are extremely high for both NIPAM and 2EHA as indicated by the crude ^{1}H NMR spectroscopy after polymerization (Figures S2–S7). [c]Theoretical molecular weight calculated according to target polymer molecular formulas = 403.7 g/mol + n × 113.2 g/mol + m × 184.3 g/mol, where n and m are the repeating units of NIPAM and 2EHA, respectively. [d]Molecular weights calculated from the ^{1}H NMR spectroscopy of the corresponding polymers. [e]All GPC data calibrated against polystyrene standards. [f]Number-average molecular weight. [g]Weight-average molecular weight. [h]Dispersity (Đ = M_w/M_n).

is formed, and vice versa.[35] Therefore, to design new RAFT polymer-based surfactants for water-in-oil HIP emulsion, the polymer needs to be soluble in the oil phase and the polymer should be low in molecular weight.

To achieve these two design principles, RAFT polymerization was used to synthesize polymers to replace the traditionally used nonionic surfactant (Sorbitan monooleate[6]) in w/o emulsions. As shown in Figure 2 and Table 1, these polymers, with dispersity below 1.5, have short polymer chain lengths (molecular weights range from 900 to 2500 g/mol) as specifically controlled via RAFT agent at the terminal of polymer chains, and these block polymers have a relatively high lipophilic portion of P2EHA to allow the solubility in oil phase; meanwhile a hydrophilic block of PNIPAM for emulsion stabilization (Figure 1). High monomer conversion for both NIPAM and 2EHA polymerization was achieved according to the crude ^{1}H NMR spectra of reactions (Table 1, Figures S2–S6), with GPC results and GPC traces of these polymers provided (Table 1, Figure S8).

In this study, PNIPAM was adopted as the hydrophilic portion of block copolymer surfactants. Short PNIPAM chains

were preferred to facilitate the dissolution of the polymer in oil. Tucker and Stevens reported molecular dynamic simulations of the thermoresponsive property of PNIPAM and the length dependence of the single chain in water.[36] They observed no transition in conformation for short chain lengths (N < 8), with a clear transition in PNIPAM conformation for chain lengths N > 11.[36] However, to date, there are no reported studies of thermoresponsiveness of PNIPAM in oil.

2.2. Instruments and Methods. *2.2.1. Nuclear Magnetic Resonance Spectroscopy (NMR).* To determine the molecular weight (calculated) of the synthesized polymers, we performed NMR spectroscopy. ^{1}H NMR spectra were obtained with 400 MHz Bruker instruments. NMR chemical shifts (δ) are reported in ppm and were calibrated against the residual solvent signal of CDCl$_3$ (δ 7.26).

2.2.1.1. Gel Permeation Chromatography (GPC)—THF Solvent System. Gel permeation chromatography (GPC) was performed on a Waters Alliance system comprising a Waters Alliance 2695 Separations Module (integrated quaternary solvent delivery, solvent degasser, and autosampler system), a Waters column heater module, a Waters 2414 RDI refractive

index detector, and a Waters PDA 2996 photodiode array detector (210 to 400 at 1.2 nm). The GPC is equipped with 4 Agilent PL-Gel columns (3 × PL-Gel Mixed C (5 μm) and 1 × PL-Gel Mixed E (3 μm) columns), each 300 mm × 7.8 mm, providing an effective molar mass range of 200 to 2 × 10^6. The solvent system used is tetrahydrofuran (THF, HPLC grade). The solvent was prepared by prefiltered through aluminum oxide (90 active neutral, 70−230 mesh) with 0.45 μm filter, and 0.1 g/L 2,6-di-*tert*-butyl-4-methylphenol (BHT) was added as an inhibitor. The filtered THF containing BHT was purged slowly with nitrogen gas and used as the eluent with a flow rate of 1 mL/min at 30 °C. The GPC columns were calibrated with low dispersity polystyrene (PS) standards (Polymer Laboratories) ranging from 580 to 7,500,000 g/mol, and molar masses are reported as PS equivalents.

2.2.2. Emulsification Procedure. Traditional emulsion binders were prepared using equal portions of kerosene and sorbitan monooleate in a stainless-steel bowl. Water containing 3 wt % sodium chloride was added in increments and mixed using an electric mixer until the desired water fraction was reached. All emulsions were prepared at room temperature (20 ± 2 °C) and stored in a refrigerator at 3−4 °C. T1 was the emulsion composition used by van Netten et al.,[6] where the emulsion formulation has been commercialized by Jord International. Although T2 and T3 contained reduced proportions of surfactant, they were created to explore the effect of minimizing surfactant concentration to align with goals of minimizing reagents. The novel RAFT emulsion binders were prepared in the same manner, with the addition of an initial step where the polymer was dissolved in the kerosene oil using a magnetic stirrer for 3 h at 400 rpm. The compositions of the emulsion binders are outlined in Table 2.

Table 2. Composition of the Traditional and RAFT Emulsion Binders

Traditional Emulsions	Kerosene Oil v%	Sorbitan Monooleate (SMO) v%	Water Volume Fraction
T1	12	12	0.76
T2	12	6	0.82
T3	12	3	0.85

RAFT Emulsions Using Polymer B	Kerosene Oil v%	RAFT Polymer wt %	Mass Polymer Per Unit Volume Oil g/mL	Water Volume Fraction
R1	12	2.5	0.21	0.86
R2	12	1.5	0.13	0.87
R3	12	0.5	0.04	0.88

2.2.3. Rheological Behavior of the Emulsion Binders. A TA Instruments Discovery HR-3 rheometer was used to measure the rheological behavior of the emulsion binders. Trios software was used to set up the methodology for the experiments. A 40 mm parallel steel plate was selected as the geometry. Three flow sweeps at 25, 32, and 40 °C were created to measure the viscosity between the applied shear rate of 0.001 and 1000 s^{-1}. Approximately 3 mL of the emulsions was placed between the plate and geometry for analysis. Experiments were performed in duplicate.

2.2.4. Optical Imaging Using Confocal Microscopy. A Leica Stellaris Laser Scanning Confocal Microscope located at Monash Centre for Nanofabrication (MCN) was used to image the shape and size of the water droplets in the emulsion binders. Nile red was prepared with isopropyl alcohol to make

a 4 μM stock solution. Prior to imaging, 20 μL of the dye stock solution was mixed with 200 μL of the emulsion on the microscope slide, and a coverslip was placed on top. The slide was inverted and placed in the microscope sample slot. The 63 × oil objective was selected, and the images were captured at an excitation wavelength of 560 nm.

ImageJ (National Institutes of Health) was used for quantification of the water droplet size distributions for all confocal images. The raw images were processed (as shown in Supporting Information Figure S9) to obtain the diameter of each water droplet.

2.2.5. Particle Size Distribution Measurements. Talc was chosen as the mineral phase to test the recovery performance of the Traditional and RAFT emulsions. Talc is naturally hydrophobic and occurs as a common gangue mineral in ore complexes, such as chalcopyrite. The particle size distribution of talc was measured using a Camsizer X2 instrument (Retsch Technology GmbH, Germany). The X-DRY module works on the principle of dynamic image analysis according to ISO 13322-2.[37] The dispersion pressure of 350 kPa was used to ensure accurate measurement of the sample powders. Measurements were repeated three times to obtain the particle size distribution.

To understand the morphology of the talc particles and to check for any natural agglomeration, scanning electron microscopy (SEM) was conducted using a JEOL JSM-IT300 operated at 10 kV and 750 × magnification.

2.2.6. Contact Angle of Powders According to the Washburn Method. A K100 Force Tensiometer (Kruss GmbH, Germany) was used to measure the wettability of the talc powder. Fresh filter paper was placed at the bottom of a sample tube, which was then filled with talc and tapped 100 times to ensure homogeneous packing of the powder bed. The powder-filled tube was suspended from the balance at the top of the unit. The tube was immersed in a perfectly wetting liquid (contact angle = 0°), which was used to determine the bed structure parameter. The process was repeated with DI water, and the increase in weight was measured with respect to time. The parameters of 6 mm/min surface detection speed, 1 mm immersion depth, and 600 s measuring time were applied in the software.
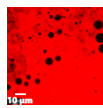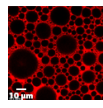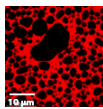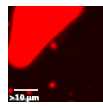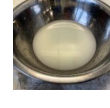
The contact angle between the powder and the water was calculated according to the condensed Washburn equation (eq 1); here, m^2/t is the mass change with respect to liquid uptake, c is the capillary constant, σ is the surface tension of liquid, θ is the contact angle between the solid powder and the liquid, and η is the viscosity of the liquid.

$$\frac{m^2}{t} = \frac{c \cdot \rho^2 \cdot \sigma \cdot \cos\theta}{\eta} \tag{1}$$

The bed structure parameter (capillary constant c) for the bulk powder was derived using the completely wetting liquid which considers the orientation of the microcapillaries and the mean capillary radius. This constant was inserted into the Washburn equation to derive the contact angle of talc with water. The contact angle measurements were repeated three times, and average was taken.

2.2.7. Talc Agglomeration Experiments. The novel RAFT emulsion binders were tested for their ability to recover talc through agglomeration. Recovery performance was measured by the proportion of talc retained in a series of sieves through which unagglomerated talc would easily pass. The talc recovery

Table 3. Summary of the Synthesized RAFT Polymers, Hydrophilic/Lipophilic Ratio, Constituent Compositions, and Confocal Microscope Images

RAFT polymer reference	Ratio of *hydrophilic-lipophilic* blocks	Polymer molecular weight g/mol	Emulsion constituent compositions	Confocal microscope image	Visual images
Polymer A	5:5	1,900	Kerosene: 5v% Polymer A: 5g Water fraction: 0.54		
Polymer B	5:10	2,800	Kerosene: 12v% Polymer A: 0.5-2.5g Water fraction: 0.85-0.87		
Polymer C	2:2	1,000	Kerosene: 5v% Polymer A: 5g Water fraction: 0.71		
Polymer D	2:5	1,150	Kerosene: 12v% Polymer A: 1-3g Water fraction: 0.85-0.87		

performance of the RAFT emulsion binders (R1, R2, R3) was compared against a benchmark, the Traditional (T1 o/w emulsion binder tested by van Netten et al.).[6] In addition, the binder stability was also compared.

Agglomeration experiments were performed inside the fumehood. A Smith & Nobel multifunction food processor was used (Supporting Information Figure S1). A slurry of talc in water (60 g in 500 mL) was prepared and conditioned for 1 min in the food processor at the lowest setting which translates to 1200 rpm. Then, 5−25 g of the emulsion binder was added using a syringe, and the contents were mixed at the same setting for 7 s. These parameters were selected based on the initial screening work carried out by Borrow.[38] The experiments were performed twice, with the data points representing the average amount of talc retained and the error bars the range. The contents were allowed 1−2 min to settle and poured into a stacked sieve tower. The mesh sizes from top to bottom were 180, 125, and 100 μm with any remaining unagglomerated particles going straight through the bottom sieve and into the bowl. The material retained in the three sieves was transferred into a tray and dried overnight in an oven at 105 °C. The dried contents were weighed, and the yield was calculated. All agglomeration experiments were performed twice.

3. RESULTS AND DISCUSSION

3.1. Screening of RAFT Polymers for Emulsification.
High internal phase (HIP) emulsions need to meet the minimum water fraction of 74.05%,[39] where the balance of 25.95% is an equal mixture of the oil and surfactant. This represents the benchmark criteria used in the traditional emulsions tested by van Netten et al.[6] and ensures lower oil requirements compared with non-HIP emulsions. The oil-surfactant contents were further reduced, and consequently,

the water content increased beyond the 0.74 water fraction for minimal oil-surfactant content in the HIP emulsions. It was reported that a water fraction of 95%, with the balance as the oil-surfactant mixture, successfully made HIP emulsions for ultrafine silica recovery.[6]

For the screening of the polymer surfactants to determine which generate suitable w/o HIP emulsions, the oil-polymer surfactant concentrations were varied. Based on the ratio of oil and surfactant in the traditional emulsion, it was hypothesized that the best opportunity for creating stable RAFT emulsions was with a high ratio of polymer surfactant to oil. However, due to the high cost of synthesizing RAFT polymers, minimizing its use was the end goal. As such, polymers able to make HIP emulsions using lower ratios of polymer to oil were preferred.

A lower and varied amount of polymer surfactant was added to the emulsions. The final water fraction that could be achieved varied for each polymer. A target water fraction of 0.85 was set to fall in between the 0.95 used in van Netten et al.[6] and the minimum 0.74 required for HIP emulsions. As with the traditional emulsions, water was added incrementally to the oil in which the RAFT polymer surfactant was already dissolved. For the emulsions with a high polymer concentration, however, there came a point where no more water could be added to the emulsion, and there was clear pooling on excess water.

It was found that Polymers A and C were not able to hold more than 25% of the expected 85% of water in the emulsion. The emulsification products were sticky in consistency and confocal microscopy showed that the water droplets in the oil phase were irregular shaped and distributed, as shown in Table 3. Interestingly, Polymer D was able to hold 100% of the expected water but formed an unstable, oil-in-water emulsion (reverse of what was expected), which separated within 30
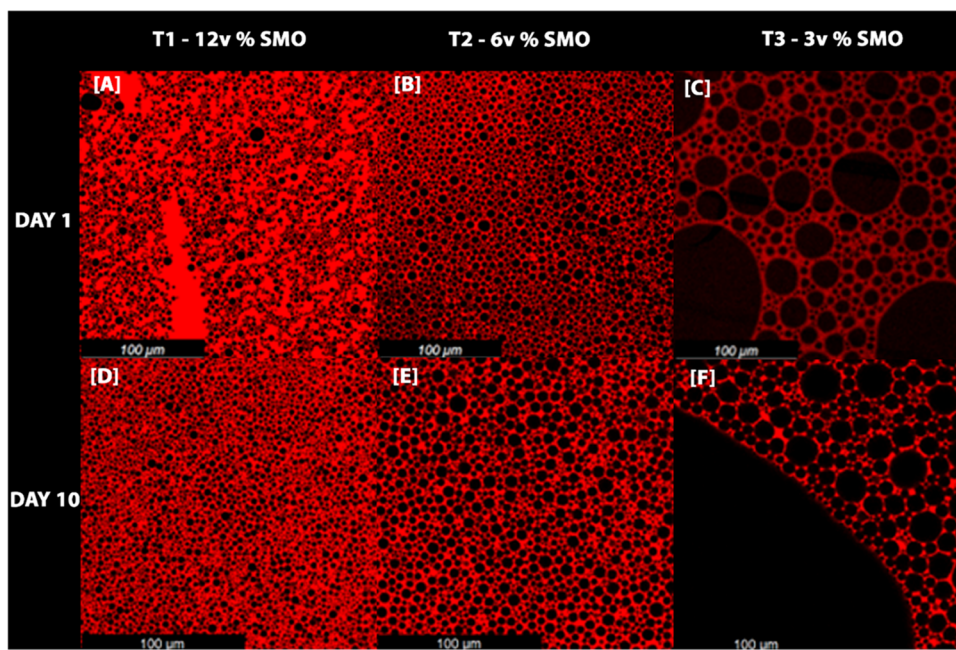
Figure 3. Confocal microscope images of water droplet size in the traditional emulsions (Top row) 12 v% kerosene oil with varying amounts of SMO: (A) T1:12 v% SMO, (B) T2−6 v% SMO, (C) T3−3 v% SMO on Day 1 (Bottom row); (D) T1−12 v% SMO, (E) T2−6 v% SMO, (F) T3−3 v% SMO on Day 10.
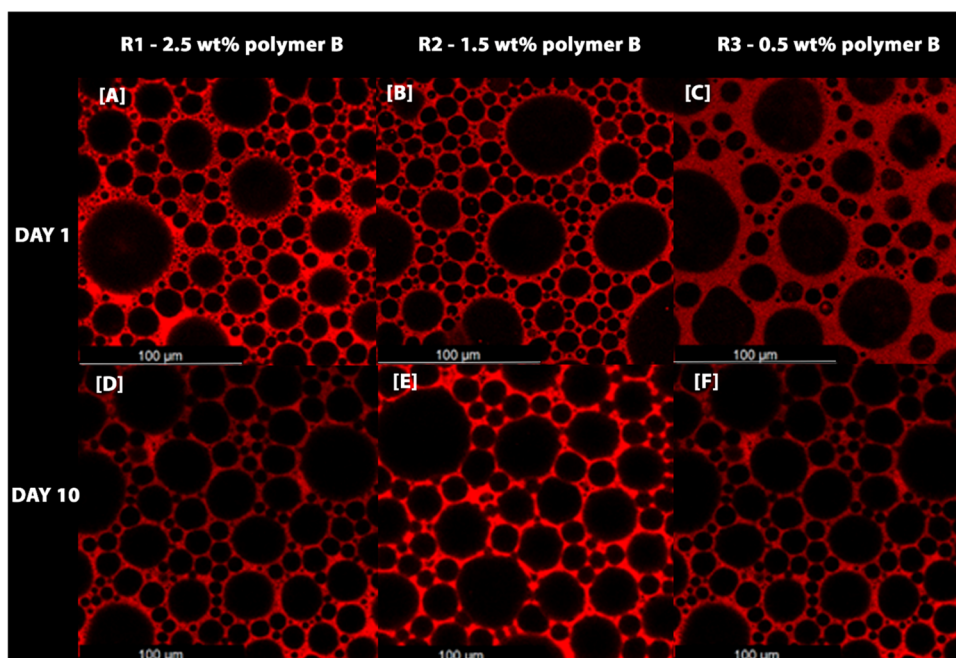
Figure 4. Confocal microscope images of water droplet size in the RAFT emulsions (top row) 12 v% kerosene oil with varying amounts of polymer B: (A) R1−2.5 wt % polymer D, (B) R2−1.5 wt % polymer B, (C) R3−0.5 wt % polymer B on Day 1; (Bottom row) (D) R1−2.5 wt % polymer B, (E) R2−1.5 wt % polymer B, (F) R3−0.5 wt % polymer B on Day 10.

min. Polymer B formed a stable water-in-oil emulsion by using the full amount of water. For this reason, polymer B was selected for characterization and performance for talc recovery. Hereafter, all references to RAFT emulsions refer to emulsions prepared with polymer B.

3.2. Stability of the w/o Emulsions by Analysis of Water Droplet Size. The purpose of the emulsion is to deliver the oil phase in water for recovery of ultrafine mineral particles. The stability of physicochemical properties over time

is important in formulating emulsions. Stable emulsions can be stored over a longer period of time and still perform effectively, improving the overall process efficiency on a large scale. An indicator of instability is Ostwald ripening, where smaller water droplets coalesce to form larger droplets and eventually break the emulsion.

In the Supporting Information, Figures S12 and S13 show visual images of the emulsions on the day of preparation and after 10 days. It can be observed that the traditional emulsions

are creamier in texture and white in appearance (Figure S12), whereas the RAFT emulsions have a fluid texture and are yellow in appearance (Figure S13).

Confocal microscopy was used to image and observe the water droplet size and distribution over time for the traditional and RAFT emulsions containing the polymer B surfactant (Figures 3 and 4, respectively). The continuous oil phase is red in the images (due to the presence, and fluorescence, of Nile red, a hydrophobic dye) and the water phase is black. Images of the emulsions were taken on the day of preparation followed by 10 days after preparation.

The interfacially adsorbed surfactant inhibits water coalescence, which impacts the droplet size depending on the amount of surfactant in the emulsion system. The size of the water droplets in the freshly prepared traditional emulsions increased from approximately 5 μm to as large as 100 μm in size as the amount of surfactant decreased in the system, as depicted in Figure 3. When the emulsion system contains equal portions of oil and surfactant (Figure 3A), the small water droplets are forced to pack closely with the short-chain lipophilic surfactant tail existing in the thin oil phase. As less surfactant is present in the system, the water droplets take up more space as there is an imbalance of surface tension at the w/o interface, reducing the stability of the emulsion. Salt is well known to stabilize water droplets and therefore w/o emulsions.[40] As sodium chloride was used to prepare the emulsions, the water droplet size appears to have only slightly increased in the 10 days after preparation, as shown in Figure 3D−F, as compared to Figure 3A−C.

Figure 4A−C illustrates the freshly prepared RAFT emulsions, which show a different water droplet size distribution in comparison to the traditional emulsions. The largest water droplets appear to be approximately 50 μm in size, surrounded by smaller water droplets of varying sizes (5−30 μm). Regardless of the amount of polymer adsorbed at the w/o interface, the large water droplet size remains consistent. Interestingly, the lowest amount of polymer (0.5 g) used in R3 (Figure 4C) has a thicker oil film compared with those of R1 and R2. Furthermore, after 10 days (Figure 4D−F), the water droplets become more closely packed, and some of the smaller water droplets have coalesced to form medium- to large-size droplets (Ostwald ripening).

The confocal microscopy revealed a feature of the RAFT emulsions that was not evident for the traditional emulsions: pockets of oil−water−oil droplets, as shown in Figure 5. These occurrences can arise for several reasons. Some examples could be during extended mixing in emulsification or due to the long block polymer structures adsorbing in different conformations at the interface as compared to the sorbitan monooleate surfactant used in the traditional emulsions. The pockets of water−oil−water droplets could contribute to extra stability of the emulsions, as the microstructure of the emulsion would break down first followed by the macrostructure over time. Bhatia et al. report that phase inversion stabilization of w/o/w emulsion, forming polymeric films, and steric stabilization all contribute to emulsion stability.[41] This attribution could be extended to the stability of the pockets of w/o/w droplets in this study. Nevertheless, the coalescence of smaller droplets into larger droplets for the RAFT emulsions suggests that although the emulsion is stable over 10 days, the stability over longer periods should also be tested.

It has been reported that the concentration of droplets in an emulsion strongly impacts the stability.[42] Quantification
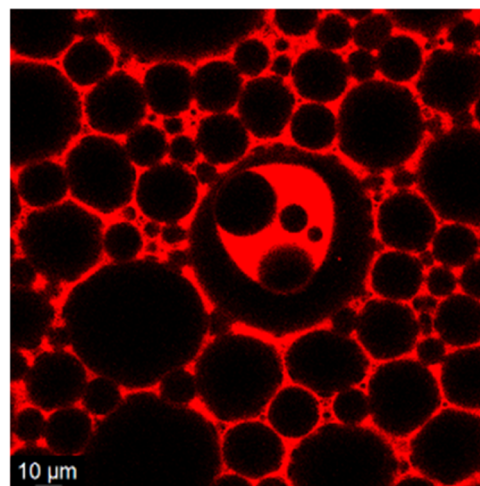

Figure 5. Confocal microscope image of o/w/o occurrence in R1 emulsion with 12 v% kerosene oil and 2.5 wt % polymer B.

analysis of the water droplet size distribution was performed on the traditional and RAFT emulsions at Day 1 and Day 10. In the Supporting Information, Figures S14 and S15 show the droplet distribution for the traditional and RAFT emulsions, respectively. At Day 1, T1 had an average water droplet size of 6 μm, whereas in comparison, R1 had an average water droplet size of 117 μm. The significantly larger water droplet size can be attributed to the longer surfactant polymer chain, as opposed to the short chains in the traditional surfactant. This trend applies to R2 and R3 with the average water droplet size at least double that in the traditional emulsions. At Day 10, the water droplet sizes increased for all emulsions apart from T1. The increase in water droplet size is due to the coalescence of the smaller water droplets over time. The percentage increase in droplet size for R1, R2, and R3 is 38, 74, and 17%, respectively. For the traditional emulsions T1, T2, and T3, the change is −10, 33, and 29%, respectively. The traditional emulsions are all monodisperse, whereas the RAFT emulsions show bimodal droplet distributions. Querol et al. have reported that the storage stability of bimodal emulsions is much higher than monodisperse emulsions,[43] despite the viscosity decreasing over time. This supports our findings, indicating that the RAFT emulsions have a higher storage stability over 10 days. Table S1 in the Supporting Information outlines the water droplet size summary in a table format.

3.3. Rheological Behavior of Fresh and Aged Emulsions. Changes in rheological behavior over time can also be an indicator of emulsion instability. The viscosity of the T1 and R1 emulsions was examined on both the day of preparation and 30 days later. Due to the thermoresponsive nature of the PNIPAM copolymer in the RAFT emulsion, three temperatures (25, 32, and 40 °C) were analyzed for both emulsions to understand and compare the viscosity. The results are shown in Figure 6. Figure 6A,C shows the viscosity as the shear rate increases for the T1 emulsion binder freshly prepared and aged, respectively. The viscosity appears to stay relatively consistent across all temperatures, with viscosity decreasing with increasing shear rate, exhibiting shear thinning behavior. Thirty days aging appears to have minimal effect on the rheological properties of this emulsion.

The rheological data for the freshly prepared R1 emulsion are shown in Figure 6B. At a low shear rate, the deviation in viscosity between the two repeats at 25 °C is largest as
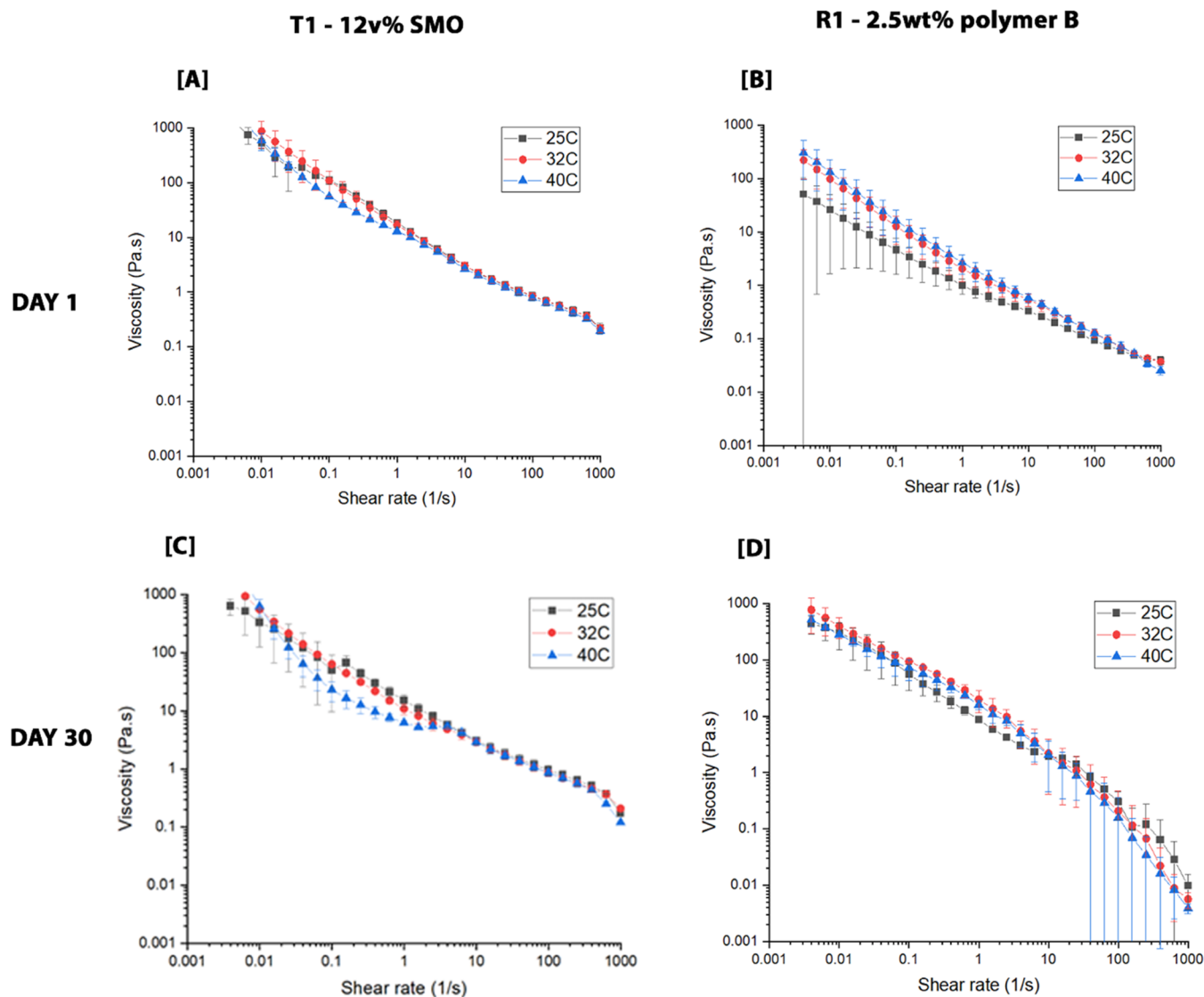
Figure 6. Plot of the apparent viscosity against shear rate for freshly prepared emulsions and aged emulsions (top row) Day of preparation (A) T1, (B) R1 (bottom row) 30 days post preparation (C) T1, (D) R1.

indicated by the larger error bars in Figure 6B. For the aged R1 emulsion in Figure 6D, there is a high deviation in viscosity between the two repeats at a high shear rate at 40 °C. Freshly prepared R1 appears to become more viscous with elevated temperature at a low shear rate. This suggests that elevating the temperature may make the agglomerated mineral−emulsion matrix more difficult to separate in subsequent downstream processing. If the temperature elevation triggered a lower viscosity, it would be possible to separate the minerals from the emulsion and recover the polymer and oil separately. Investigation of whether the polymer adsorbs to the mineral system and the strength of that adsorption interaction is an important consideration.

The traditional emulsions (both fresh and aged) used in this study have a high viscosity at low shear, which we believe is the ideal environment for minerals processing ultrafine particles. On the other hand, the fresh RAFT emulsion is less viscous by an order of magnitude at low shear, and its viscosity increases to the same value as the traditional emulsion with aging. Both traditional emulsions exhibit preferable rheological properties for mineral processing, while the RAFT emulsion tended to

exhibit these preferred properties with time. For a stable emulsion, the immiscible water and oil must remain in the system without a change for as long as possible. Ultimately, the surfactants leave the system, breaking the water−oil interface and leaving behind a less effective emulsion binder. In contrast, the RAFT emulsions show a stable and larger water droplet size, as with time, it is only the smaller water droplets that coalesce, thus forming a relatively uniform water droplet distribution.

The reproducibility of the traditional emulsion appears to be consistent, whereas the RAFT emulsions show variability. This could be accounted for by the size and degree of polymerization of the hydrophilic and lipophilic polymer chains. By introducing branched molecular structures, the conformation and orientation under applied shear and elevated temperatures would have an impact on the viscosity. Thus, the short-chained sorbitan monooleate surfactant does not display significant variability in comparison, as its short chain would be completely immersed at the oil/water interface and does not change conformation over time in the emulsion.

Ideally in industry, a lower shear rate would be preferred as it would require lower revolutions per minute, which corresponds to lower energy and therefore lower costs. The collisions in the blender promote growth by layering to form a larger agglomerate. The agglomerates will break down if a high shear rate is applied, or here is an extended mixing and collision time. Iveson and Litster reported a growth regime map for liquid-bound agglomerates, where the agglomerate liquid content was measured as the maximum pore saturation.[44] Agglomerate deformation and consolidation were used to predict the agglomerate growth behavior. Powder-binder systems that are highly deformable and quickly consolidating will grow steadily with time, but highly viscous fluids were associated with slow consolidation and induction growth, which can end in sudden and rapid agglomeration, which is hard to control. In another study, Rough et al. investigated the binder viscosity on particle agglomeration in a low-shear mixer.[45] The growth rate increased with an increase in binder viscosity up to a maximum viscosity of 100 mPa s, where the agglomerate formation was by layering mechanism. With binder viscosity of greater than 100 mPa s, the agglomerate growth was found to be by coalescence. Therefore, it can be reasonable to suggest that high-viscosity emulsions would perform best to retain particles and form agglomerates, while a low-shear process would be beneficial for industry from an economical perspective. The traditional emulsions meet this criterion as expected.

The fresh RAFT emulsion appears to have a deviation in the viscosity at 25 °C at low shear. This could be partly due to the PINPAM instability. The viscosity for the aged RAFT emulsion does not deviate at low shear at any of the tested temperatures. This could be attributed to the halo of smaller water droplets that coalesced to form a uniform water droplet distribution over time and the o/w/o pockets that also coalesced over time. However, at 40 °C with high shear, the viscosity begins to fail. This could be indicative that the PNIPAM dissolved in oil begins to change conformation at this point. This is a very promising result, as the RAFT emulsions appear to be slightly responsive to changes in thermal environment, containing only five repeating units of the PNIPAM hydrophilic block polymer. Reports in the literature indicate that PNIPAM polymers with greater than 10 repeating units begin to show thermal response in water,[36] but to the authors' knowledge, this has not been tested in organic solvents. The oil-soluble nature of our polymer may account for differences in thermoresponsiveness.

3.4. Characterization of Talc Mineral Particles. A talc mineral particle system was selected for testing the efficiency of the emulsion binders for the agglomeration tests. The particle size distribution is shown in the Supporting Information Figure S10 and a summary is presented in Table 4. The mean particle diameter was measured to be 15 μm; this is consistent with the ultrafine minerals that are below the optimal size range of 15 to 150 μm for particle capture by froth flotation[46] and therefore

Table 4. Particle Size Distribution of the Talc Feed Showing the Surface Area Mean $D_{(3,2)}$, Volume Moment Mean $D_{(4,3)}$, and the Particle Size Associated to Each Percentile Mean (D_{10}, D_{50}, and D_{90})

powder (μm)	$D_{(3,2)}$	$D_{(4,3)}$	D_{10}	D_{50}	D_{90}
talc	6.5	20.1	3.0	15.3	44.3

represents the size fraction that is of most interest to the minerals processing industry for recovery via alternative means. Scanning electron microscopy (Supporting Information Figure S11) confirmed the predominant talc morphology to be platelike, with many of the particles below 10 μm. No evidence of natural agglomeration was observed.

To hydrophobicity of the talc mineral in aqueous and nonaqueous media was measured according to the Washburn test. The contact angle of talc was determined to be 83° in water, as shown in Figure 7. This is in line with the literature
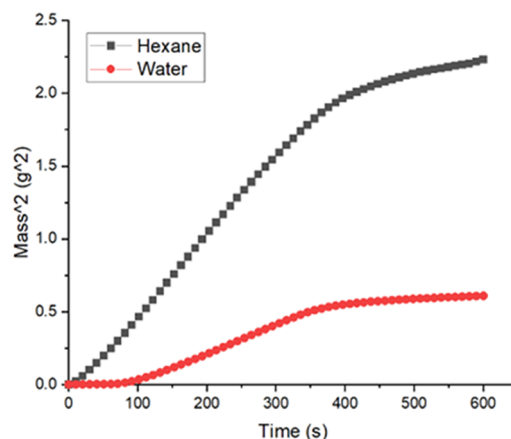

Figure 7. Mass change of talc powder with respect to time in deionized water (wetting agent) and *n*-hexane (nonwetting agent) and the measured contact angle.

that reports the talc contact angle to vary between 83 and 88° depending on the degree of powder bed packing.[47] The oil in the emulsion binder is hypothesized to bond to the hydrophobic surface of talc, assisting in the agglomerate recovery.

3.5. Agglomeration of Hydrophobic Talc Mineral Particles. Agglomeration tests were performed using the three traditional and three RAFT emulsions described in Table 2. The amount of emulsion added to the 12 wt % of talc suspension varied from 5 to 25 g. The talc recovery using the traditional emulsion is shown in the top row of Figure 8 (A−C). The stacked sieves retained three different size fractions of agglomerated talc. The mass retained in the three sieves was measured individually and then combined, and the total talc recovery was calculated.

For all agglomeration experiments using traditional emulsions, there was a layer of froth that formed on top of the mineral suspension and captured some of the talc particles. The froth and associated talc were retained in the top sieve (180 μm). In agglomeration experiments using T1, the top sieve (180 μm) retained the most mineral particles in the froth, the middle sieve (125 μm) captured some of the particles, while the bottom sieve (100 μm) captured the least. In contrast, T2 and T3 did not retain nearly as much talc in the froth in the top sieve (5−30% for T2 & T3 compared to 20−70% for T1), and the majority of the talc was retained in the middle sieve. For all three traditional emulsions and almost all quantities of emulsion, the bottom sieve (100 μm) captured <20% of the talc, and in most cases, <5% of the talc. All traditional emulsions achieved a total recovery of approximately 80% of the talc. The remaining 20% of the talc was retained in the liquid phase that passed through the sieves.
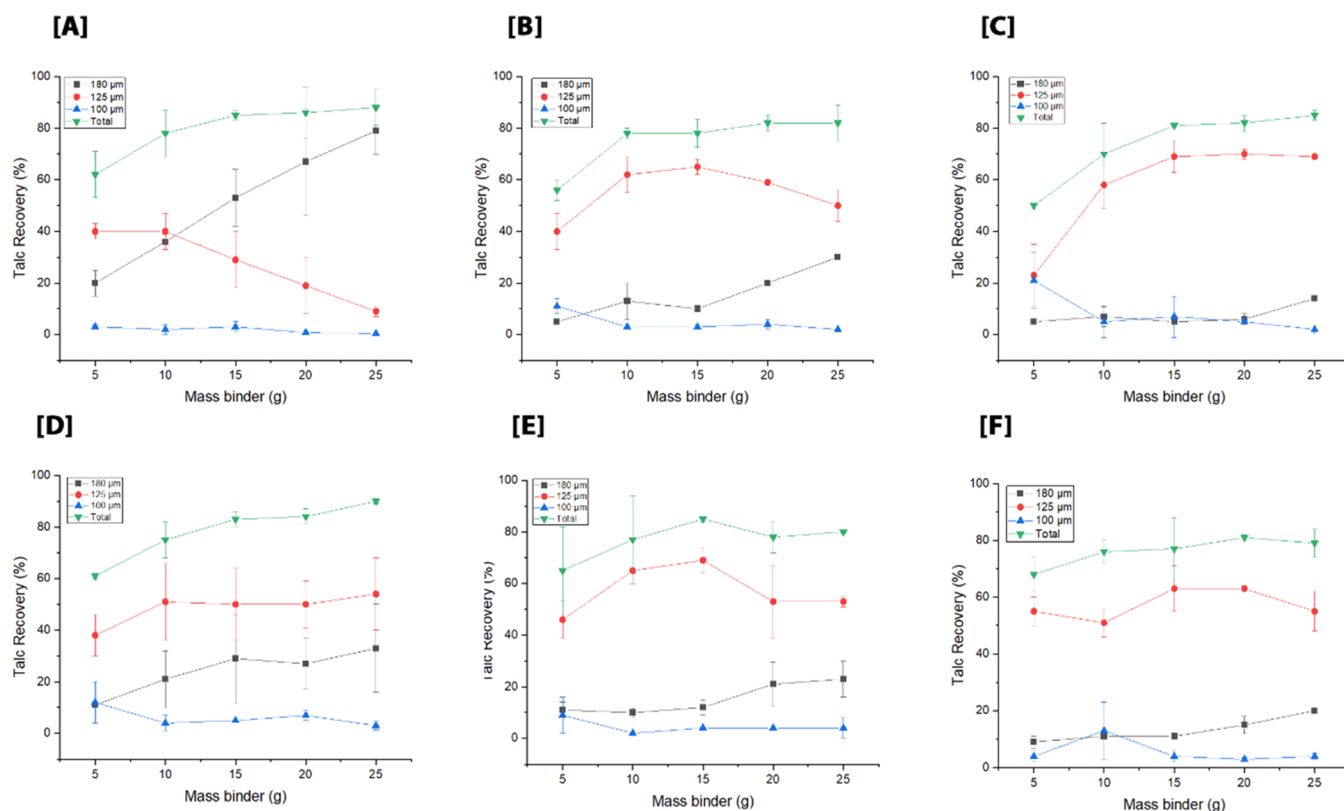
Figure 8. Talc mineral percentage yield recovered against mass of emulsion binder added: (Top row) Traditional emulsion (A) T1−12 v% SMO, (B) T2−6 v% SMO, (C) T3−3 v% SMO. (Bottom row) RAFT emulsion D (D), R1−2.5 wt % polymer B, (E) R2−1.5 wt % polymer B, (F) R3− 0.5 wt % polymer B. All emulsions contain 12 v% kerosene oil.
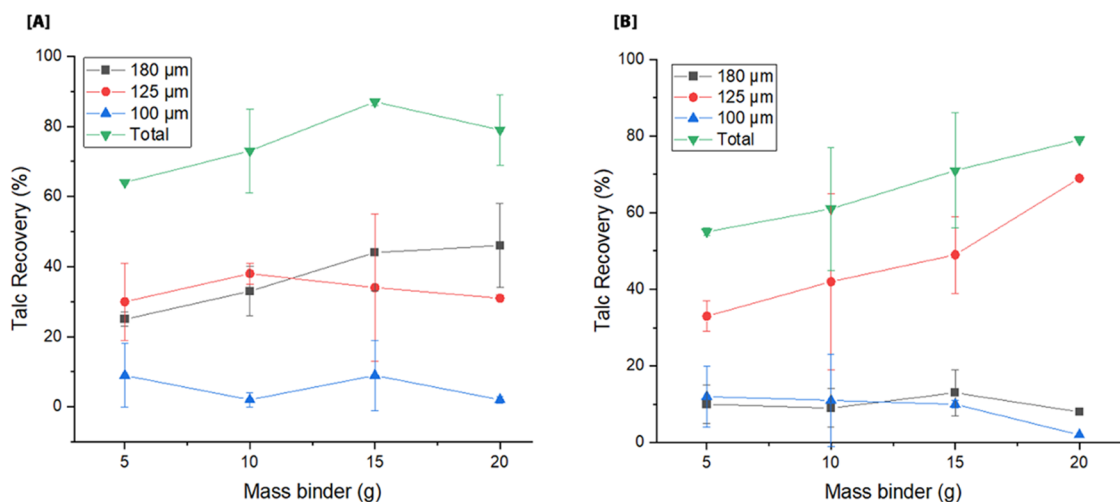
Figure 9. Percentage yield of talc recovered against mass of emulsion binder added using 30-day old emulsion binder: (A) T1:12 v% kerosene and 12 v% SMO and (B) R1:12 v% kerosene oil and 2.5 wt % polymer B.

It can be seen in Figure 8A that 10 g of T1 represents a crossover point above which more talc was retained in the top sieve than and middle sieves. A similar trend can be observed for T2 and T3 at much higher emulsion binder masses. These observations can be explained by the emulsion formulation and the mineral recovery method. T1 contained the highest amount of surfactant at 12 v%. On breaking of the emulsion binder during the applied shear, the large amount of surfactant present likely caused the froth formation, which in turn captured much of the talc. As the amount of emulsion binder used was increased, the amount of froth, and in turn talc

captured in the froth and retained in the 180 μm sieve, increased.

T2 & T3 contained lower proportions of surfactant, so the primary mechanism of talc recovery was via the formation of small agglomerates between 125 and 180 μm in size. The lower amounts of surfactant prevented the generation of excessive froth, although the trend toward more froth, and more recovery in the 180 μm sieve, can be seen as the mass of the emulsion binder is increased. The bottom row in Figure 8D−F illustrates the talc recovery using the RAFT emulsions. The RAFT emulsions contain 12 v% kerosene oil, and the mass of

polymer D varied between 2.5 and 0.5 g (R1−R3). The R1 emulsion produced the highest overall talc recovery at 90%. R2 and R3 had an approximate average talc recovery of 80%, close to the talc recovery with the traditional emulsions. The RAFT emulsions produced less froth, and the majority of the talc was recovered as small agglomerates in the middle sieve (125 μm). As a result of the lack of froth, the R1 trend line did not have a cross point, as with the T1 emulsion binder.

The results indicate that on the breaking of the emulsion, depending on the amount of surfactant present, there are two mechanisms resulting in talc recovery that occur simultaneously: (1) On formation of a froth, some talc is captured within the structure, and (2) on delivery of oil, some talc is agglomerated into small particles. While both scenarios can be considered as recovery due to the emulsion binder, in an industry application, they would require different strategies and equipment for the collection of the talc and therefore consideration as to which is preferable when deciding which emulsion binder composition is preferred.

From the perspective of minimizing reagent use while maximizing recovery, it is noteworthy that the traditional emulsion binders all reach a plateau in talc recovery at ∼80% by 15 g binder (i.e., 20 and 25 g of binder do not increase the amount of talc recovered). While this also appears to be the case for R2 and R3, R1 demonstrates an increasing trend in talc recovery to ∼90% at 25 g emulsion binder. The increased recovery for the RAFT-based emulsion R1, beyond the traditional emulsion recovery, is an encouraging result. Further work should be considered to determine if 90% recovery can be exceeded with an increase in the mass of the emulsion binder. There may also be scope to optimize the emulsion binder composition to explore whether a composition intermediate of R1 & R2 could result in 90% recovery at lower binder mass.

3.6. Effect of Emulsion Aging on Talc Recovery. T1 and R1 aged for 30 days were used for talc agglomeration to compare the effectiveness of the surfactant and polymer over time. The results are presented in Figure 9. NB - In Figure 9B, the 20 g data points represent a single test only.

Figure 9A shows that while the overall talc recovery was similar at ∼80% for fresh and aged T1 emulsion binder, the proportion of talc captured in the top and middle sieves is different, with a reduced proportion captured in the top sieve for all masses of emulsion binder. Similar to the aged T1 emulsion, Figure 9B shows that the aged R1 emulsion results in a higher proportion of the talc retained in the middle sieve than for the fresh emulsions. However, the maximum total talc recovered using aged R1 is lower than for the fresh emulsion, at ∼75% compared to 90%.

This data suggests that 30 days of aging has different effects on two types of emulsions. For the T1 emulsion, aging does not appear to have affected the ability to deliver the oil that causes the agglomeration; hence, talc recovery is still high. However, the ability of the surfactant to produce froth has been reduced. This could suggest that aged traditional-style emulsions could be used to minimize the frothing effect and increase the proportion of mineral agglomerated. The effect of aging on the R1 emulsion appears to be to reduce its effectiveness at agglomerating the talc. Considering the coalescence of water droplets observed using the confocal microscope, this could potentially be attributed to early stages of emulsion separation and kerosene oil evaporation.

For best performance, it is recommended to use freshly prepared emulsions, where the polymer/surfactant is able to exert greater control over water droplet size, and therefore stability, of the emulsions. Further work is required to determine whether the aging effect on the RAFT polymers can be reduced.

3.7. Applicability of RAFT Emulsions to Mineral Processing. *3.7.1. Recovery of Talc.* Of all of the emulsion binders tested, the highest talc recovery was achieved using 25 g of fresh R1 emulsion binder. An improvement of ∼10% talc recovery was seen as compared to that of the best performing traditional emulsion binder. This is a significant increase, and further experiments should be conducted to determine if the trend observed in increasing talc recovery with increasing binder mass extends beyond the 25 g tested. These results clearly indicate that polymers engineered through the RAFT process are suitable to replace traditional surfactants in HIP emulsions.

The stability of the binder over time is important, as it ensures the water droplets are uniformly distributed and their size remains relatively stable in the continuous oil phase over time. The aged T1 emulsions did not recover as much talc in the froth compared to the fresh counterpart. This may be linked to the slight evaporation of volatile kerosene oil from the emulsion system over time, reducing the hydrophobic nature of the emulsion and hence the recovery of the talc. This hypothesis could also be applied to RAFT emulsions. The minerals processing industry would benefit from emulsions that are as stable as the RAFT emulsions, however, with the optimization of talc recovery.

With respect to the temperature sensitivity of the RAFT emulsions, we found that the low number of repeating PNIPAM units may not be enough to observe a thermal response at low shear. This is consistent with recent findings by Tucker and Stevens that suggest for full temperature responsiveness a minimum of 10 repeating PNIPAM units are needed,[36] although their study used water-soluble polymers. However, for the first time, we report oil-soluble PNIPAM polymers coupled with block copolymer P2EHA show "some" activity with a change in temperature under applied shear. While this is not enough temperature responsiveness to enable recovery of the polymer after the mineral agglomeration process, it represents a starting point in the development of stimuli-responsive polymers to replace surfactants, and work is ongoing to improve responsiveness and therefore recovery.

It is of note that highly viscous emulsions are desirable for more effective agglomeration in combination with the presence of the oil. Such thermally responsive polymers inside emulsion systems must be stored in cool environments to prevent the surpassing of the lower critical solution temperature (32 °C), changing the conformation of the PNIPAM polymer. This could lead to the emulsion not performing as anticipated.

Future steps to help optimize the recoverability of RAFT polymers from the emulsion system include increasing the number of repeating PNIPAM units (N > 10) to observe a clear transition in conformation of the polymer and therefore viscosity at elevated temperatures. Furthermore, the selectivity of the emulsions with respect to recovering a certain type of mineral can be explored. RAFT polymers are expensive to synthesize; however, optimization of their functionality to improve the selectivity and recoverability at a laboratory scale could allow us to develop emulsions that outweigh the initial associated costs.

3.7.2. Use of Talc as a Model Mineral System. While it has been reported that mineral powders with a contact angle of as low as 60 to 80° are suitable for processing,[48] with a contact angle of ~83°, talc holds challenges for use in minerals agglomeration mainly due to its variable surface charge and morphology. The morphology of talc powder is sheet-like, where the predominant basal plane holds a surface charge that varies from positive to negative with increasing pH, while the edges are negative across all pH values.[49] This challenge was overcome by employing a nonionic polymer that does not rely on the ionic interaction for binding with the talc. Furthermore, the sheet-like morphology means the suspension forms a thick layer of mineral cake when passed through a sieve with mesh size on the upper end of the particle size distribution (80 μm). To overcome this challenge, a stacked tower method was employed by using sieves with a mesh size range between 100 and 180 μm to ensure the individual talc particles go straight through the finest sieve. Moreover, the stacked tower method allowed investigation of the aggregate size formed after the addition of emulsion. To further test the efficacy of the RAFT emulsion binders and explore the mechanisms by which the agglomeration differs from traditional emulsion binders, a hydrophobic mineral system that does not have the inherent complexities of talc could be chosen, although this would take the experiments further away from the complex realities of industrial minerals processing.

3.7.3. Recovery of the Polymer. The RAFT polymers in this study had intentionally been synthesized to incorporate a thermoresponsive block to allow for ultimate polymer recyclability. The PNIPAM block transitions from hydrophilic to hydrophobic above its LCST temperature of 32 °C.[50] The recyclability concept for this study is in line with a study reported by Li et al. for the development of pH-responsive magnetic nanospheres via RAFT synthesis for the application of Pickering emulsions.[51] They found that upon the introduction of magnetism, the emulsion was demulsified and unable to be restored to its original form. This allowed the magnetic polymers to be recovered, recycled and reused. In our work, the temperature-responsive nature of the surfactant polymer allows the ability to exploit the emulsion behavior. We reported the rheological properties of the emulsion to understand its behavior at elevated temperatures. Ideally, increasing the temperature would transition the conformational structure of the polymer, releasing the mineral particles attached to it. We have proven the basis for this work in this study to show that the synthesized RAFT polymer is suitable for the emulsification and recovery of talc mineral particles. The future work will optimize the polymer for recyclability and reuse in subsequent experiments.

4. CONCLUSIONS

RAFT polymerization was employed to synthesize various oil-soluble polymers with PNIPAM block as the thermoresponsive block. Polymer B with a hydrophilic–lipophilic block ratio of 5–10 performed well in both emulsification to the novel w/o emulsion and high talc mineral recovery (90%), outperforming by almost 10% the talc recovery of the traditional emulsion at 25 g of emulsion. For the RAFT emulsions, a larger proportion of the talc was recovered in the agglomerate phase, whereas for the traditional emulsions, a significant proportion of the talc was associated with the foam phase.

With respect to the emulsion stability, the RAFT emulsion droplet sizes were bigger and more stable due to a halo of smaller droplets and pockets of o/w/o emulsions that coalesce with time. Overall, considering the 6 different emulsion compositions tested, the talc recovery using RAFT emulsions is like that of the research benchmark. This work is an important first step in demonstrating the suitability of polymer surfactants engineered for recoverability via the RAFT process for use in HIP emulsions for minerals processing. The future work required to optimize the polymer includes improving the polymer functionality to be more selective with the type of mineral recovered, increasing the number of repeating PNIPAM chains to distinguish between thermally responsive profiles, and optimizing the polymer structure so it improves the minerals recovery.

■ ASSOCIATED CONTENT

Data Availability Statement

All data generated during this study are included in this published article.

Ⓢ Supporting Information

The Supporting Information is available free of charge at https://pubs.acs.org/doi/10.1021/acsomega.3c05270.

Characterization data for the polymers, minerals, and emulsions (PDF)

■ AUTHOR INFORMATION

Corresponding Authors

Ellen M. Moon − *School of Engineering, Deakin University, Waurn Ponds, VIC 3216, Australia; ARC Centre of Excellence for Enabling Eco-efficient Beneficiation of Minerals;* ⓞ orcid.org/0000-0002-1779-8587; Email: ellen.moon@deakin.edu.au

San H. Thang − *School of Chemistry, Monash University, Clayton Campus, VIC 3800, Australia; ARC Centre of Excellence for Enabling Eco-efficient Beneficiation of Minerals;* ⓞ orcid.org/0000-0003-2629-3895; Email: san.thang@monash.edu

Authors

Negin Amini − *School of Engineering, Deakin University, Waurn Ponds, VIC 3216, Australia; ARC Centre of Excellence for Enabling Eco-efficient Beneficiation of Minerals*

Bo Fan − *School of Chemistry, Monash University, Clayton Campus, VIC 3800, Australia; ARC Centre of Excellence for Enabling Eco-efficient Beneficiation of Minerals;* ⓞ orcid.org/0000-0003-3067-9627

Tina Hsia − *School of Chemistry, Monash University, Clayton Campus, VIC 3800, Australia; ARC Centre of Excellence for Enabling Eco-efficient Beneficiation of Minerals*

Karen Hapgood − *Swinburne University, Hawthorn, VIC 3122, Australia; ARC Centre of Excellence for Enabling Eco-efficient Beneficiation of Minerals*

Complete contact information is available at:
https://pubs.acs.org/10.1021/acsomega.3c05270

Author Contributions

‖N.A. and B.F. contributed equally.

Notes

The authors declare no competing financial interest.

■ ABBREVIATIONS

T1, traditional emulsion 1; T2, traditional emulsion 2; T3, traditional emulsion 3; R1, RAFT polymer emulsion 1; R2, RAFT polymer emulsion 2; R3, RAFT polymer emulsion 3; RAFT polymerization, reversible addition—fragmentation chain transfer polymerization; CDPA, 4-cyano-4-((((dodecylthio)carbonothioyl)thio) pentanoic acid; NMR, Nuclear Magnetic Resonance; 2EHA, 2-ethylhexyl acrylate; LCST, lower critical solution temperature; w/o emulsion, water-in-oil emulsions; HIP, high internal phase; SMO, Sorbitan Monooleate

■ REFERENCES

(1) Nagaraj, D.; Farinato, R. Evolution of flotation chemistry and chemicals: a century of innovations and the lingering challenges. *Miner. Eng.* 2016, 96-97, 2−14.

(2) Van Berkel, R. Eco-efficiency in the Australian minerals processing sector. *J. Cleaner Prod.* 2007, 15 (8−9), 772−781.

(3) Sis, H.; Chander, S. Reagents used in the flotation of phosphate ores: a critical review. *Miner. Eng.* 2003, 16 (7), 577−585.

(4) DataIntelo. *Mining Collectors Market Research Report*, 2023; p 112.

(5) Mehrotra, V.; Sastry, K.; Morey, B. Review of oil agglomeration techniques for processing of fine coals. *Int. J. Miner. Process.* 1983, 11 (3), 175−201.

(6) van Netten, K.; Borrow, D. J.; Galvin, K. P. , Fast Agglomeration of ultrafine hydrophobic particles using a high-internal-phase emulsion binder comprising permeable hydrophobic films. *Ind. Eng. Chem. Res.* 2017, 56 (38), 10658−10666.

(7) Hornn, V.; Park, I.; Ito, M.; Shimada, H.; Suto, T.; Tabelin, C. B.; Jeon, S.; Hiroyoshi, N. Agglomeration-flotation of finely ground chalcopyrite using surfactant-stabilized oil emulsions: Effects of co-existing minerals and ions. *Miner. Eng.* 2021, 171, No. 107076.

(8) Sahasrabudhe, G.; DeIuliis, G.; Davy, J.; Galvin, K. Selective and ultrafast agglomeration of chalcopyrite by a water in oil emulsion binder. *Miner. Eng.* 2021, 167, No. 106900.

(9) van Netten, K.; Moreno-Atanasio, R.; Galvin, K. P. Fine particle beneficiation through selective agglomeration with an emulsion binder. *Ind. Eng. Chem. Res.* 2014, 53 (40), 15747−15754.

(10) Pitt, K.; Peña, R.; Tew, J. D.; Pal, K.; Smith, R.; Nagy, Z. K.; Litster, J. D. Particle design via spherical agglomeration: A critical review of controlling parameters, rate processes and modelling. *Powder Technol.* 2018, 326, 327−343.

(11) Bemer, G. G. Agglomeration in Suspension: A study of mechanisms and kinetics. 1979.

(12) Iveson, S. M.; Litster, J. D.; Hapgood, K.; Ennis, B. J. Nucleation, growth and breakage phenomena in agitated wet granulation processes: a review. *Powder Technol.* 2001, 117 (1−2), 3−39.

(13) Fu, Z.; Liu, M.; Xu, J.; Wang, Q.; Fan, Z. Stabilization of water-in-octane nano-emulsion. Part I: Stabilized by mixed surfactant systems. *Fuel* 2010, 89 (10), 2838−2843.

(14) John, J.; Bhattacharya, M.; Raynor, P. C. Emulsions containing vegetable oils for cutting fluid application. *Colloids Surf., A* 2004, 237 (1−3), 141−150.

(15) Ghavidel, N.; Fatehi, P. Interfacial and emulsion characteristics of oil−water systems in the presence of polymeric lignin surfactant. *Langmuir* 2021, 37 (11), 3346−3358.

(16) Kang, W.; Xu, B.; Wang, Y.; Li, Y.; Shan, X.; An, F.; Liu, J. Stability mechanism of W/O crude oil emulsion stabilized by polymer and surfactant. *Colloids Surf., A* 2011, 384 (1−3), 555−560.

(17) Moad, G. Mechanism and Kinetics of Dithiobenzoate-Mediated RAFT Polymerization—Status of the Dilemma. *Macromol. Chem. Phys.* 2014, 215 (1), 9−26.

(18) Chiefari, J.; Chong, Y.; Ercole, F.; Krstina, J.; Jeffery, J.; Le, T. P.; Mayadunne, R. T.; Meijs, G. F.; Moad, C. L.; Moad, G.; Rizzardo, E.; Thang, S. H. Living free-radical polymerization by reversible addition− fragmentation chain transfer: the RAFT process. *Macromolecules* 1998, 31 (16), 5559−5562.

(19) Fan, B.; Wan, J.; McKay, A.; Qu, Z.; Thang, S. H. Facile synthesis of well-controlled poly (1-vinyl imidazole) by the RAFT process. *Polym. Chem.* 2020, 11 (35), 5649−5658.

(20) Mei, G.; Zheng, Y.; Fu, Y.; Huo, M. Polymerization-induced self-assembly of random bottlebrush copolymers. *Polym. Chem.* 2022, 13 (37), 5389−5396.

(21) Wan, J.; Fan, B.; Putera, K.; Kim, J.; Banaszak Holl, M. M.; Thang, S. H. Polymerization-induced hierarchical self-assembly: from monomer to complex colloidal molecules and beyond. *ACS Nano* 2021, 15 (8), 13721−13731.

(22) Fan, B.; Wan, J.; Zhai, J.; Chen, X.; Thang, S. H. Triggered degradable colloidal particles with ordered inverse bicontinuous cubic and hexagonal mesophases. *ACS Nano* 2021, 15 (3), 4688−4698.

(23) Fan, B.; Wan, J.; Zhai, J.; Teo, N. K. S.; Huynh, A.; Thang, S. H. Photoluminescent polymer cubosomes prepared by RAFT-mediated polymerization-induced self-assembly. *Polym. Chem.* 2022, 13 (29), 4333−4342.

(24) Xu, K.; Fan, B.; Putera, K.; Wawryk, M.; Wan, J.; Peng, B.; Banaszak Holl, M. M.; Patti, A. F.; Thang, S. H. Nanoparticle Surface Cross-Linking: A Universal Strategy to Enhance the Mechanical Properties of Latex Films. *Macromolecules* 2022, 55 (13), 5301−5313.

(25) Thompson, K. L.; Mable, C. J.; Cockram, A.; Warren, N. J.; Cunningham, V. J.; Jones, E. R.; Verber, R.; Armes, S. P. Are block copolymer worms more effective Pickering emulsifiers than block copolymer spheres? *Soft Matter* 2014, 10 (43), 8615−8626.

(26) Wang, J.; Han, Y.; Li, J.; Wei, J. Selective adsorption of thiocyanate anions using straw supported ion imprinted polymer prepared by surface imprinting technique combined with RAFT polymerization. *Sep. Purif. Technol.* 2017, 177, 62−70.

(27) Lockwood, A. P.; Wadsley, G.; Warren, N. J.; Peakall, J.; Webber, G. B.; Wanless, E. J.; Rhodes, D.; Barnes, M.; Harbottle, D.; Hunter, T. N. Amphiphilic block copolymers as dual flocculation-flotation agents for rapid solid-liquid separation of radioactive wastes. *Sep. Purif. Technol.* 2023, 323, No. 124387.

(28) Heskins, M.; Guillet, J. E. Solution properties of poly (N-isopropylacrylamide). *J. Macromol. Sci., Chem.* 1968, 2 (8), 1441−1455.

(29) Kohori, F.; Sakai, K.; Aoyagi, T.; Yokoyama, M.; Sakurai, Y.; Okano, T. Preparation and characterization of thermally responsive block copolymer micelles comprising poly (N-isopropylacrylamide-b-DL-lactide). *J. Controlled Release* 1998, 55 (1), 87−98.

(30) Liu, M. S.; Taylor, C.; Chong, B.; Liu, L.; Bilic, A.; Terefe, N. S.; Stockmann, R.; Thang, S. H.; De Silva, K. Conformational transitions and dynamics of thermal responsive poly (N-isopropyla-crylamide) polymers as revealed by molecular simulation. *Eur. Polym. J.* 2014, 55, 153−159.

(31) Zhang, P.; Liu, F.; Liao, Q.; Yao, H.; Geng, H.; Cheng, H.; Li, C.; Qu, L. A microstructured graphene/poly (N-isopropylacrylamide) membrane for intelligent solar water evaporation. *Angew. Chem., Int. Ed.* 2018, 57 (50), 16343−16347.

(32) Haq, M. A.; Su, Y.; Wang, D. Mechanical properties of PNIPAM based hydrogels: A review. *Mater. Sci. Eng., C* 2017, 70, 842−855.

(33) Pasban, S.; Raissi, H. PNIPAM/Hexakis as a thermosensitive drug delivery system for biomedical and pharmaceutical applications. *Sci. Rep.* 2022, 12 (1), No. 14363.

(34) Lee, M. C.; Tan, C.; Ravanfar, R.; Abbaspourrad, A. Ultrastable water-in-oil high internal phase emulsions featuring interfacial and

biphasic network stabilization. *ACS Appl. Mater. Interfaces* **2019**, *11* (29), 26433−26441.

(35) Kramer, S.; Cameron, N. R.; Krajnc, P. Porous polymers from high internal phase emulsions as scaffolds for biological applications. *Polymers* **2021**, *13* (11), 1786.

(36) Tucker, A. K.; Stevens, M. J. Study of the polymer length dependence of the single chain transition temperature in syndiotactic poly (N-isopropylacrylamide) oligomers in water. *Macromolecules* **2012**, *45* (16), 6697−6703.

(37) ISO. *Particle size analysis - Image analysis methods - Part 2: Dynamic image analysis methods*; International Organization for Standardization, 2021−12; p 53.

(38) Borrow, D. J. *Beneficiation of Dense Minerals through Agglomeration*; University of Newcastle Australia, 2019.

(39) Lissant, K. J. *Emulsions and Emulsion Technology*; M. Dekker, 1974; Vol. *6*.

(40) Taylor, P. Ostwald ripening in emulsions. *Adv. Colloid Interface Sci.* **1998**, *75* (2), 107−163.

(41) Bhatia, N.; Pandit, S.; Agrawal, S.; Gupta, D. A review on multiple emulsions. *Int. J. Pharmaceutical Erudition* **2013**, *3* (2), 22−30.

(42) Mcclements, D. J. Critical review of techniques and methodologies for characterization of emulsion stability. *Crit. Rev. Food Sci. Nutr.* **2007**, *47* (7), 611−649.

(43) Querol, N.; Barreneche, C.; Cabeza, L. F. Storage stability of bimodal emulsions vs. monomodal emulsions. *Appl. Sci.* **2017**, *7* (12), 1267.

(44) Iveson, S. M.; Litster, J. Growth regime map for liquid-bound granules. *AIChE J.* **1998**, *44* (7), 1510−1518.

(45) Rough, S.; Wilson, D.; Bayly, A.; York, D. Mechanisms in high-viscosity immersion−granulation. *Chem. Eng. Sci.* **2005**, *60* (14), 3777−3793.

(46) Mankosa, M.; Kohmuench, J.; Christodoulou, L.; Yan, E. Improving fine particle flotation using the StackCell(raising the tail of the elephant curve). *Miner. Eng.* **2018**, *121*, 83−89.

(47) Galet, L.; Patry, S.; Dodds, J. Determination of the wettability of powders by the Washburn capillary rise method with bed preparation by a centrifugal packing technique. *J. Colloid Interface Sci.* **2010**, *346* (2), 470−475.

(48) Atkin, R.; Craig, V. S.; Wanless, E. J.; Biggs, S. Mechanism of cationic surfactant adsorption at the solid−aqueous interface. *Adv. Colloid Interface Sci.* **2003**, *103* (3), 219−304.

(49) Yin, X.; Gupta, V.; Du, H.; Wang, X.; Miller, J. D. Surface charge and wetting characteristics of layered silicate minerals. *Adv. Colloid Interface Sci.* **2012**, *179-182*, 43−50.

(50) Lutz, J.-F.; Akdemir, Ö.; Hoth, A. Point by point comparison of two thermosensitive polymers exhibiting a similar LCST: is the age of poly (NIPAM) over? *J. Am. Chem. Soc.* **2006**, *128* (40), 13046−13047.

(51) Li, K.; Dai, H.; Li, J.; Zhang, Q.; Wang, B. Development of recyclable pH-responsive magnetic nanospheres via RAFT polymerization and their application in Pickering emulsions. *Colloids Surf., A* **2022**, *648*, No. 129281.